ACS APPLIED MATERIALS & INTERFACES

Research Article

www.acsami.org

Sol–Gel Preparation of Hydrophobic Silica Antireflective Coatings with Low Refractive Index by Base/Acid Two-Step Catalysis

Shuang Cai,[†] Yulu Zhang,[†] Hongli Zhang,[†] Hongwei Yan,[‡] Haibing Lv,*[,‡] and Bo Jiang*[,†]

[†]Key Laboratory of Green Chemistry & Technology, College of Chemistry, Sichuan University, Chengdu 610064, China

[‡]Research Center of Laser Fusion, China Academy of Engineering Physics, Mianyang 621900, China

Supporting Information

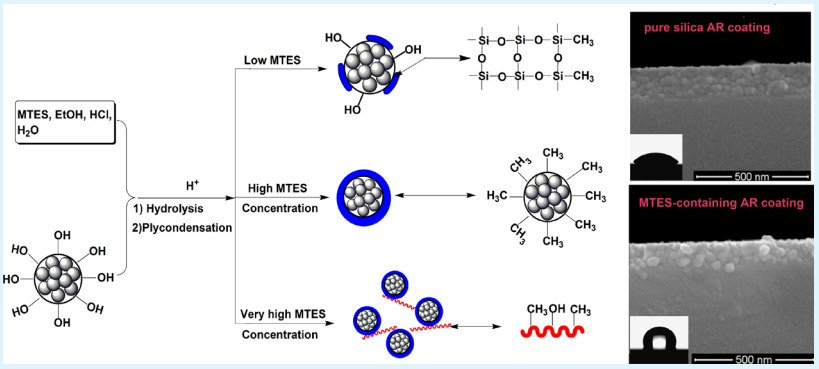

ABSTRACT: Hydrophobic antireflective coatings with a low refractive index were prepared via a base/acid-catalyzed two-step sol–gel process using tetraethylorthosilicate (TEOS) and methyltriethoxysilane (MTES) as precursors, respectively. The base-catalyzed hydrolysis of TEOS leads to the formation of a sol with spherical silica particles in the first step. In the second step, the acid-catalyzed MTES hydrolysis and condensation occur at the surface of the initial base-catalyzed spherical silica particles, which enlarge the silica particle size from 12.9 to 35.0 nm. By a dip-coating process, this hybrid sol gives an antireflective coating with a refractive index of about 1.15. Moreover, the water contact angles of the resulted coatings increase from 22.4 to 108.7° with the increases of MTES content, which affords the coatings an excellent hydrophobicity. A "core–shell" particle growth mechanism of the hybrid sol was proposed and the relationship between the microstructure of silica sols and the properties of AR coatings was investigated.

KEYWORDS: *TEOS, MTES, two-step, core–shell*

1. INTRODUCTION

Porous silica antireflective (AR) coatings have been widely reported recently. The advantages in thermal resistance, high transmission, and selectivity make them well-suited for a variety of practical applications like optical devices and energy-related application such as solar cells, laser system, optical filters, cathode ray tubes, and shop windows.[1−7] AR coatings are usually used to reduce transmission losses. Desired AR coatings can achieve effectually zero reflection at a particular wavelength when its refractive index equals $(n_a n_s)^{1/2}$, where n_a and n_s are the refractive indices of air and substrate, respectively.[8,9] Porous silica coatings prepared by the sol–gel process have been now widely used as quarter-wave layers, because their refractive index could present as low as 1.23, which approximates to the square root of 1.52 that is the index of many types of optical substrates. Although these conventional single-layer quarter-wave coatings can in theory lead to zero reflection at a single wavelength, broadband AR coatings are often very desirable for many applications. However, because of the unavailability of simple optical materials with even lower refractive indices than 1.23, such broadband AR coatings have not been industrialized on a large scale. Since the lowest refractive index that can be achieved in dense materials is 1.38 (that of MgF_2), nanoporous materials have emerged and rapidly developed.[10]

As a prospective method for preparation of nanoporous materials, the sol–gel process has attracted a good deal of attention because of its advantages of superior homogeneity, low cost, low processing temperature, and simple operation process.[11] Nevertheless, hydroxyl groups existing on the pure silica particles and the high porosity (about 50–60%) afford these sol–gel AR coatings with poor hydrophilicity that limits greatly their uses in humidity environment. The adsorption of water directly decreases the porosity of the AR coating, which results in an increase in refractive index, which leads to a dramatic decrease in optical performance of the AR coating. Although many attempts have been made to improve the hydrophobicity of silica AR coatings by introducing organic molecules or polymers bearing hydrophobic groups into the

Received: April 8, 2014
Accepted: June 30, 2014
Published: June 30, 2014

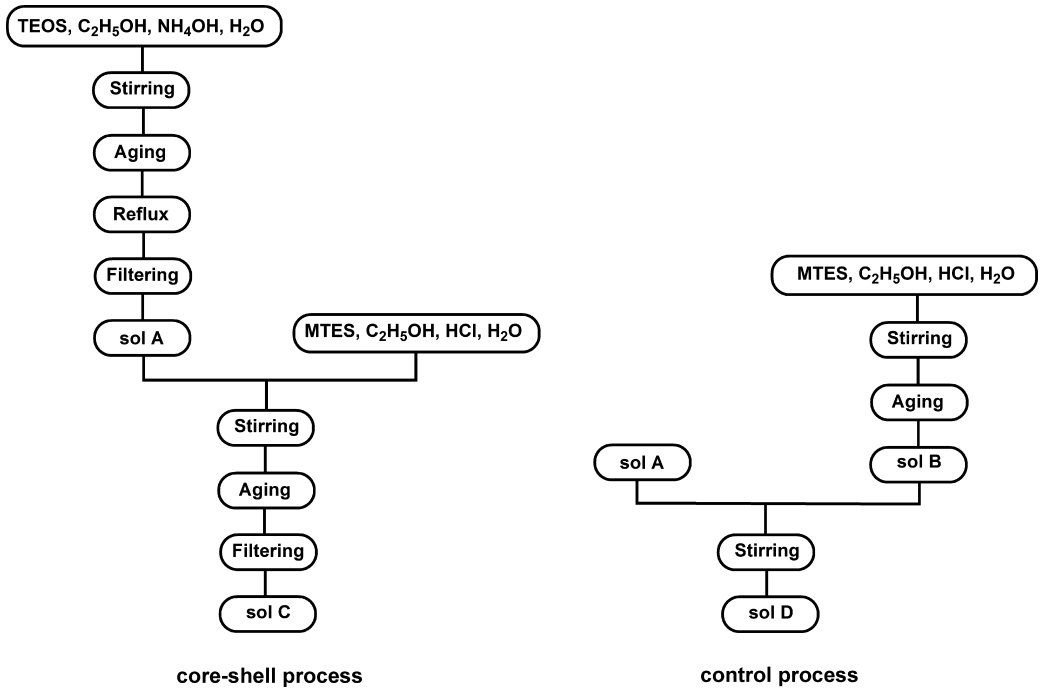

Figure 1. Procedure for preparation of the silica sols.

coating.[13−16] Still, no one can give consideration to both the very-low refractive index and good hydrophobicity.

In this paper, we report a base/acid two-step catalyzed sol−gel process, using tetraethoxysilane (TEOS) and methyl triethoxysilane (MTES) as precursor respectively in the corresponding step, to form a layer of methyl cladding hydrophobic shell on the initial base-catalyzed silica particles, which gives an hydrophobic AR coatings with low-refractive. A core−shell particle growth mechanism of the hybrid sol was proposed.

2. EXPERIMENTAL PROCEDURES

Figure 1 shows the process for the preparation of silica sols. These hybrid sols were made from TEOS (kermel, highly pure, China), MTES (kermel, highly pure, China), ethyl alcohol (C_2H_5OH, EtOH), deionized water, $NH_3{\cdot}H_2O$ (13.4 mol/L), and HCl, so as the controlled trial which was made by preparing AR coatings from the mixture of base-catalyzed TEOS sol and acid-catalyzed MTES Sol.

2.1. Preparation of Silica Sols. First, base-catalyzed silica sol was made by mixing a solution of EtOH, TEOS, H_2O, and $NH_3{\cdot}H_2O$. The molar ratio of TEOS:H_2O:EtOH:NH_3 was 1:3.25:37.6:0.17. The mixtures were first stirred for 2 h at 30 °C and then aged at 25 °C for 7 days. After that, it was refluxed for 24 h to remove ammonia and finally filtered through a 0.22 μm PVDF filter prior to use. The final concentration of SiO_2 in the sol was 3% by weight. The sol was noted as Sol A. Second, MTES were added in sol A in proportions to give 0, 10, 20, 30, 40, 50, 60, 70, 80, 90, and 100% of the total silica sol with the molar ratio of MTES, ETOH, HCl, and H_2O was 2.5:93.5:1:1.02 × 10^{-3}:1, assuming that 1 mol of TEOS or MTES gives 1 mol of SiO_2 and H_3C-$SiO_{1.5}$ (polymethylsilsesquioxane), respectively. These hybrid sols were also stirred at 30 °C for 2 h and aged for 7 days to allow MTES to react fully. These final products noted as Sol C were filtered through a 0.22 μm PVDF filter prior to use.

2.2. Preparation of Controlled Trial Sols. EtOH, MTES (kermel, high pure, China), H_2O and $NH_3{\bullet}H_2O$ (13.4 mol/L) was first mixed and stirred for 2 h at 30 °C. The molar ratio of MTES, EtOH, H_2O and HCl was 2.5:93.5:1:1.02 × 10^{-3}. This pure acidic MTES sol was noted as Sol B. After aging at 25 °C for 7 days, Sol A and Sol B were simply mixed with different weight ratio. The mixture of Sol A and Sol B was noted as Sol D, which was used as the controlled trial.

2.3. Preparation of AR Coatings. BK7 glass substrates were properly cleaned before dip-coating. The silica sols were deposited on those substrates using the dip-coating process at different withdrawal rates (from 75 to 400 mm min^{-1}) to make center wavelength of the coatings around 550 nm (room temperature 20−30 °C; relative humidity < 20%). All silica films were heat-treated at 160 °C for 8 h before tests.

2.4. Characterization of Silica Coatings. Infrared absorption spectra of samples 0, 30, 50, and 70% were analyzed by FTIR (Bruker Tensor 27).

To determine particle size and distribution, the silica sols were analyzed by dynamic light scattering (DLS, Malvern Nano-ZS, wavelength of 632.8 nm) at 25 °C. Ten measurements were done on each sample to calculate the average and standard deviation.

The refractive indices of the AR coatings were determined by ellipsometry (SENTECH SE850 UV, error limits ≤2%) at 550 nm.

Cross-sectional scanning electron microscopy (SEM) images of silica coatings were taken using a S-4800 field-emission scanning electron microscope operated at 5KV.

Water contact angle was measured with a Krüss DSA100 (Germany) instrument (error limits ≤1%) .

Antireflective durability was tested by exposing to humid laboratory air (room temperature: 20−30 °C; relative humidity> 90%) for two months.

The visible light transmittance spectra of the AR coatings was measured by an UV−vis (Mapada, UV-3100PC, transmittance error ≤0.2%, wavelenght ≤0.1 nm).

3. RESULTS AND DISCUSSION

3.1. Structure of Sol Particles Characterized by IR Spectroscopy. Figure 2 shows the FTIR spectra of pure silica 0%, 30%, 50%, 70% hybrid silica xerogel. All samples present two absorption bands at 1069 and 800 cm^{-1}, corresponding to bending and stretching vibrations of Si−O−Si bond, respectively. The absorption band at 955 cm^{-1} is attributed to the hydroxyl group of Si−OH. The intensity of which weakens with the increase of acid-catalyzed silica concentration.

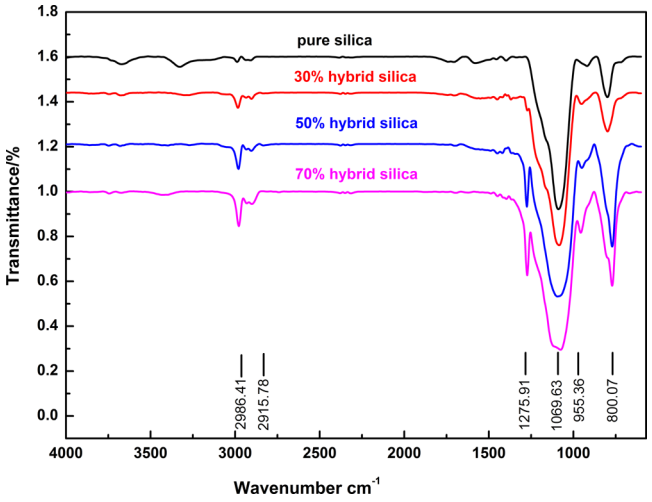

Figure 2. FTIR spectra of pure silica 0, 30, 50, and 70 hybrid silica sols.

Table 1. Particle Size and Its Distribution of the Hybrid Sols

Sol C (%)	particle size (nm)	PdI
0	12.9 ± 1.2	0.13−0.19< 0.2
10	15.7 ± 1.5	0.09−0.13< 0.2
20	18.0 ± 1.7	0.08−0.15< 0.2
30	28.0 ± 2.9	0.09−0.14< 0.2
40	30.5 ± 3.1	0.10−0.14< 0.2
50	31.1 ± 3.2	0.09−0.16< 0.2
60	35.1 ± 3.5	0.12−0.17< 0.2
70	36.8 ± 3.7	0.10−0.18< 0.2
80	37.1 ± 4.0	0.08−0.15< 0.2
90	40.1 ± 4.1	0.11−0.17< 0.2

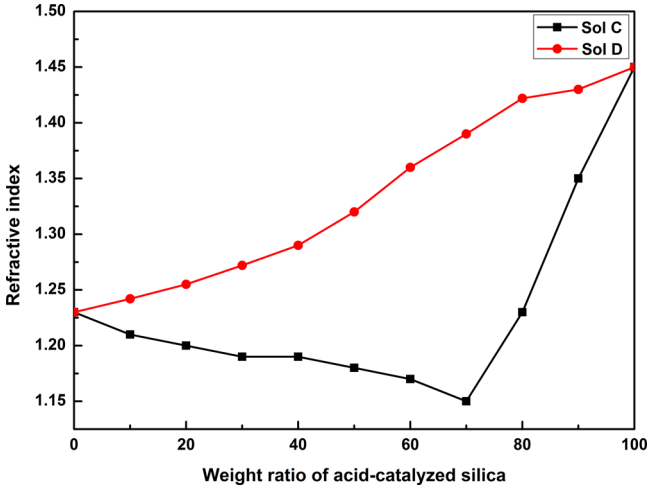

Figure 3. Change in the refractive index as a function of the weight ratio of acid-catalyzed silica.

The adsorption bands of C−H in methyl groups exhibit at 2986 and 2915 cm^{-1}, and enhance with the increase of acid-catalyzed silica concentration. For hybrid silica samples, an additional absorption band appears at 1275 cm^{-1}, corresponding to the characteristic Si-CH_3 stretching vibrations. These results demonstrate that the hydroxyl groups on the silica particles were replaced and the condensation between MTES and silica particles occurred effectively.

3.2. Particle Size Investigated by DLS. A controlled aggregation mechanism, proposed by Zukoski and co-workers to describe the growth of silica particles, is widely recognized in sol−gel science.[17,18] During the growth, the subparticles aggregated to form particles, and once these particles reached a certain size, stable particle size and colloid sols were obtained due to the surface charges. Table 1 shows the hybrid silica particle size and their distribution. As we can see, the pure base-catalyzed silica particle size is 12.9 nm, and that of hybrid ones could reach to 35.0 nm with the increase of the acid-catalyzed MTES proportion; moreover, the PDI (polydispersity index) of all the samples are lower than 0.2, demonstrating a good monodispersity. It is obvious that the addition of acid-catalyzed MTES only produced larger size particles with diameters of several tens of nanometres, but did not change the distribution. These hybrid silica particle size are still much smaller than the wavelength of visible light, Mie and Rayleigh scattering can be neglected. Otherwise, the good monodispersity guarantees the homogeneity of derived AR coatings.

3.3. Refractive Indices of the Coatings. It is well-known that the refractive index of a porous silica AR coating decreases with the increase of porosity in coating.[19] We reported previously a base/acid two-step catalyzed sol−gel process of silica AR coating using TEOS as a single precursor.[5] During the second step with an acidic catalyst, the hydrolysis of TEOS tends to form linear chains on the silica particles formed during the initial base catalyzed condensation that will fill among the spherical particles during the coating process. This reduce the porosity of the film, leading to an increase of the refractive index. In that report the refractive index of the coatings increased with the increase of the weight ratio of acid-catalyzed silica. In this study, MTES was used in the subsequent acid-catalyzed step. If the same filling process takes place, an increase in the refractive index of the coating should be observed with the increase proportion of the acid-catalyzed MTES. In fact, a different and interesting change of the refractive index was observed. As showed in Figure 3, the refractive index of the coatings prepared from base/acid two-step catalyzed silica sol (Sol C) decreased with the increase of the weight ratio of acid-catalyzed MTES at first and increased suddenly when the concentration of acid-catalyzed MTES exceeded 70%.

3.4. Particle Growth Mechanisms. All kind of silicon alkoxides with pendant groups were used to prepare AR silica coatings. Research on the relationship between sol−gel process and the properties of the silica coating has been done partly. MTES is one of commonly used trifunctional organosilanes as a single precursor or a coprecursor with TEOS to investigate the hydrolysis kinetics[20] and the effect of pendant groups[21] via some relatively complex process. However, this simple base/acid two-step catalyzed sol−gel process using TEOS and MTES system has long been neglected. As we previously reported,[5] when TEOS is catalyzed by $NH_3{\cdot}H_2O$, the growth of silica sol is biased toward spherically expanding particles giving the derived coatings high porosity and a low refractive index 1.23 as shown in Figure 4a. When MTES is used as single precursor under acid condition, the growth of silica sol tends to form liner chains as shown in Figure 4b, thus the derived coatings are dense and possess a high refractive index. It is noteworthy that the rate of MTES hydrolysis is much higher than its condensation due to steric hindrance effect.[22] In the TEOS base/MTES acid two-step catalyzed method, spherical silica particles are formed in the first base-catalyzed step with a large

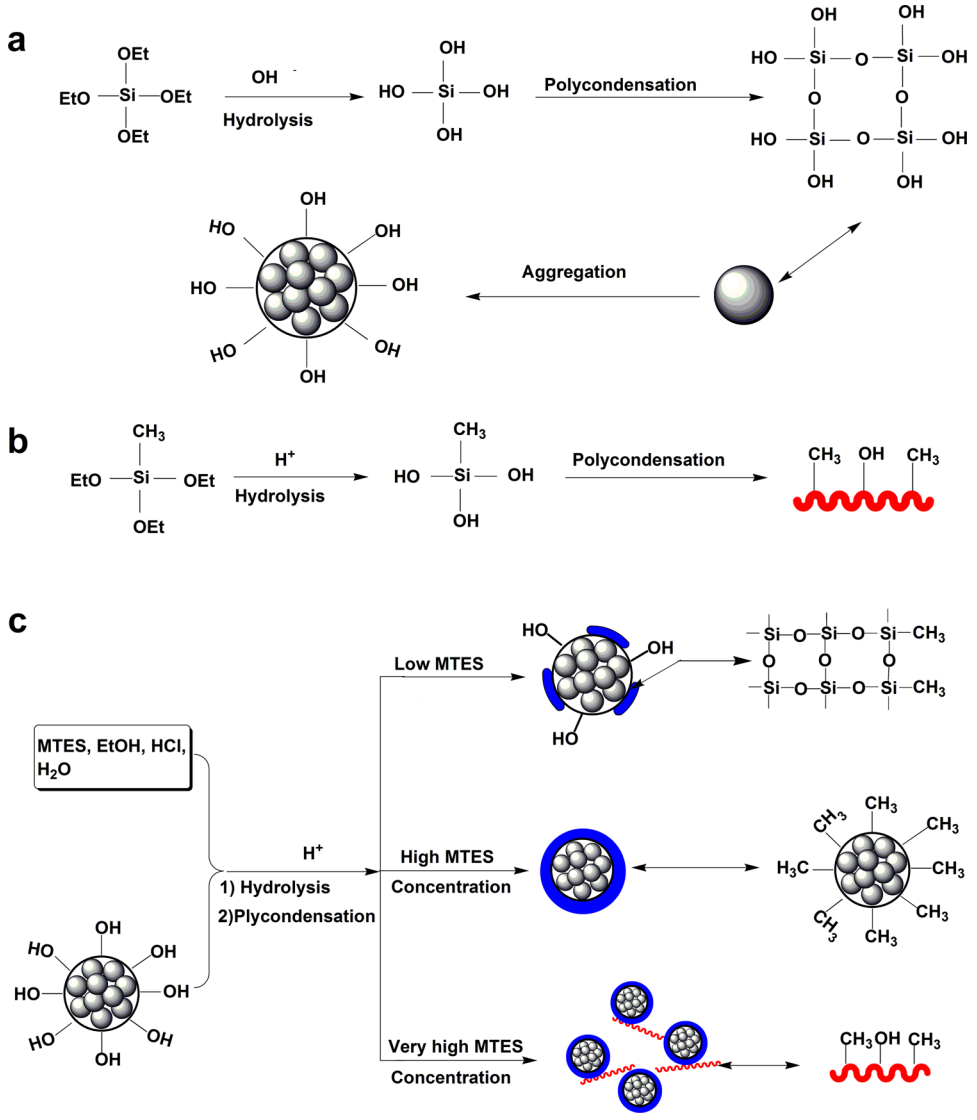

Figure 4. (a) Growth model of the particle under base catalysis; (b) growth model of the particle under acid catalysis; (c) growth model of the particle in hybrid sol.

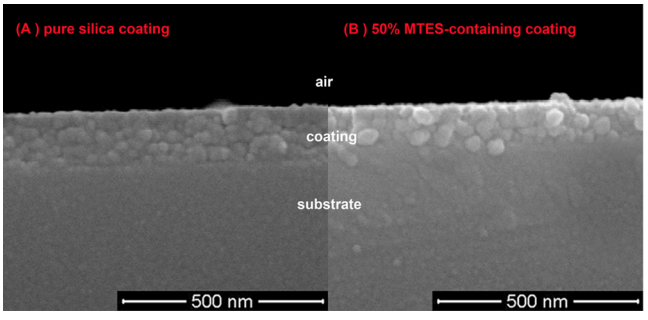

Figure 5. SEM images of (A) pure silica coating and (B) 50% MTES-containing coating.

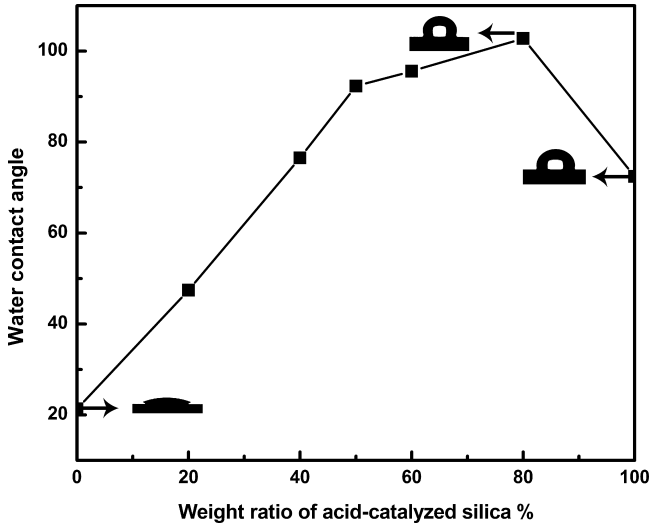

Figure 6. Water contact angle values versus the weight ratio of acid-catalyzed silica.

amount of hydroxyl groups on the surface; when MTES is added into this silica sol with an acid catalyst, the hydrolysis reaction will be initiated immediately, whereas the condensation may take place in two different ways: self-condensation of hydrolysis products of MTES; or co-condensation between the hydrolysis products and the spherical silica particles in the sol. The self-condensation reaction may proceeds much slowly

dx.doi.org/10.1021/am501972y | ACS Appl. Mater. Interfaces 2014, 6, 11470−11475

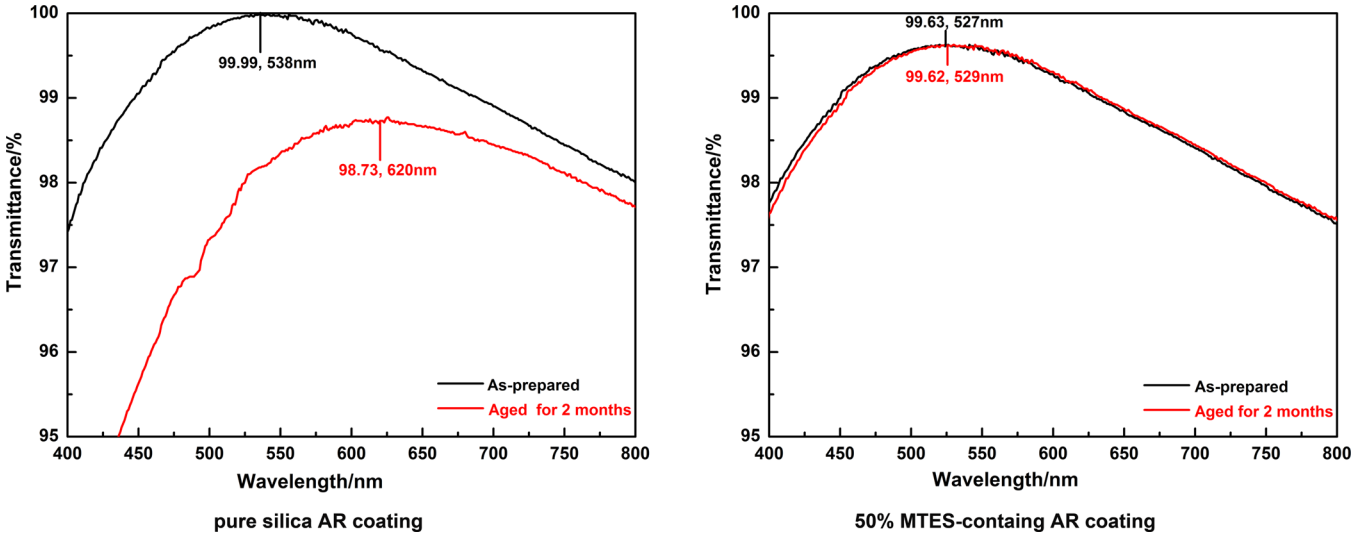

Figure 7. Change in visible light transmittance spectra of the AR coatings as a function of test time.

owing to the above-mentioned steric hindrance effect. Therefore, three different ways of sol particles growth mechanism, base on the "core" of base-catalyzed silica particle, are proposed as shown in Figure 4 C. When the proportion of acid-catalyzed MTES is low, MTES hydrolysis and co-condense on the base-catalyzed silica particles, and only a small part of silicon hydroxyl groups Si−OH transform to Si−O−$SiCH_3$. However, these small amount of incorporated methyl groups $-CH_3$ do rouse the change in particle size and surface charge of initial particles. Along with the increase of MTES proportion, more $-CH_3$ replace the −OH on initial particles, enlarging the particle size and decreasing the surface charge further, which are exactly two of main factors that decrease the refractive index of coatings.[23,24] When the proportion of acid-catalyzed MTES comes to a value high enough, the Si−O−$SiCH_3$ will spread all over the initial particle's surface and on the other word, the "core-shell" structure reached integrated and saturated. In this case, the refractive index of derived coatings presents lowest 1.15, as shown in Figure 3. Over the turning-point around 70%, filling model works that results in an abrupt increase in refractive index.

For comparison, a series of physical mixtures of base-catalyzed TEOS sol and acid-catalyzed MTES sol was prepared and dip-coated. Figure 3b shows that the refractive index of the coatings from the mixed sol increases gradually with the increase of acid-catalyzed MTES sol proportion. There obviously occurs a filling process for coatings with these physical sol mixtures, providing another evidence for the "core−shell" mechanism of the TEOS base/MTES acid two-step catalyzed hybrid sol.

3.5. Cross-Sectional SEM Images of Silica Coatings. Figure 5 displays the cross-sectional SEM image of pure silica coating and 50% MTES-containing coating. The pure silica and MTES-containing silica nanoparticles are both densely packed to form a single-layer film with a thickness of around 100 nm. The average diameter of the pure silica coating's particle is about 12 nm, and that of the 50% MTES-containing coating is around 35 nm. This result is in good agreement with the data by particle size analysis. The nanoparticles of pure silica coating are packed closer than that of 50% MTES-containing coating, which means that the void space in the film of 50% MTES-containing coating is larger than that of pure silica coating. The larger void space gives the MTES-containing coating a lower refractive index.

3.6. Hydrophobicity. Hydrophobicity is an essential property of the coating that directly concerns with its humidity-resistance. Pure base-catalyzed silica AR coatings are highly hydrophilic and unstable in a humid environment because of the −OH group on the surface. The hydrophobic nature of the silica thin film measured by water contact angle is closely linked to AR durability of the coating. As the hydrophobic methyl groups are incorporated on the surface of silica particles during the acid-catalyzed MTES in the second step, the water contact angle of the derived coatings reaches a maximum value of 108.7° as shown in Figure 6. Maximum contact angle of 108.7° was also significantly larger than that of pure MTES coating of 78.7° which can be explained by the core−shell particle growth mechanism. According to the core−shell structure of TEOS/MTES hybrid sols, more methyl groups were oriented toward the outer surface, giving the coating a higher hydrophobicity than pure MTES coating. Similar phenomena have also been observed by Ma Y and co-workers.[25]

Figure 7 shows the deviation of the visible light transmittance spectra of pure and 50% MTES-containing AR coatings. After keeping in a sealed container with a 95% relative humidity at room temperature for two months, the maximum transmittance of the pure silica AR coating decreases dramatically from 99.99 to 98.73%, whereas that of the 50% MTES-containing AR coatings only decreases from 99.62 to 99.60%. It is clearly that antireflective durability of these MTES-containing AR coatings was dramatically improved. The adsorption of water from wet ambience was effectively prevented by the incorporation of methyl groups introduced in the acidic step which affords these MTES-containing AR coatings a better optical durability in a humid environment.

4. CONCLUSION

Antireflective coating with low refractive index and enhanced humidity-resistance was prepared by a TEOS base/MTES acid two-step catalyzed sol−gel process. The addition of acid-catalyzed MTES in the base-catalyzed silica sol enlarges the particle size from 12.9 to 35.0 nm, the new hybrid sol gives a hydrophobic coating with a water contact angle of 108.7°. The

value of refractive index of the AR coatings can reach as low as 1.15. A core−shell particles growth mechanism was proposed that explains well the properties of the hybrid sols and the coatings. This hydrophobic coating may have great application potential and good development prospective.

■ ASSOCIATED CONTENT

Supporting Information

This material is available free of charge via the Internet at http://pubs.acs.org.

■ AUTHOR INFORMATION

Corresponding Authors

*E-mail: haibinglv@163.com (H.L.).
*E-mail: jiangbo@scu.edu.cn (B.J.).

Notes

The authors declare no competing financial interest.

■ ACKNOWLEDGMENTS

The authors gratefully acknowledge the support from the Natural Science Foundation of China "Project J1103315" supported by NSFC.

■ REFERENCES

(1) Kim, Y. S.; Kusakabe, K.; Morooka, S.; Yang, S. M. Preparation of Microporous Silica Membranes for Gas Separation. Korean. *J. Chem. Eng.* **2001**, *18*, 106−112.
(2) Asaeda, M.; Yamasaki, S. Separation of Inorganic/Organic Gas Mixtures by Porous Silica Membranes. *Sep. Purif. Technol.* **2001**, *25*, 151−159.
(3) Prevo, B. G.; Hon, E. W.; Velev, O. D. Assembly and Characterization of Colloid-Based Antireflective Coatings on Multi-crystalline Silicon Solar Cells. *J. Mater. Chem.* **2007**, *17*, 791−799.
(4) Zhang, L.; Qiao, A.; Zheng, M.; Huo, Q.; Sun, J. Rapid and Substrate-independent Layer-by-Layer Fabrication of Antireflection- and Antifogging-Integrated Coatings. *J. Mater. Chem.* **2010**, *20*, 6125−6130.
(5) Ye, H. P.; Zhang, X. X.; Zhang, Y. L.; Ye, L. Q.; Xiao, B.; Lv, H. B.; Jiang, B. Preparation of Antireflective Coatings with High Transmittance and Enhanced Abrasion-Resistance by a Base/Acid Two-Step Catalyzed Sol−Gel Process. Sol. Energy. *Mater. Sol. Cells* **2011**, *95*, 2347−2351.
(6) Prene, P.; Priotton, J. J.; Beaurain, L.; Belleville, P. Preparation of a Sol-Gel Broadband Antireflective and Scratch-Resistant Coating for Amplifier Blastshields of the French Laser LIL. *J. Sol−Gel Sci. Technol.* **2000**, *19*, 533−537.
(7) Penard, A. L.; Gacoin, T.; Boilot, J. P. Functionalized Sol−Gel Coatings for Optical Applications. *Acc. Chem. Res.* **2007**, *40*, 895−902.
(8) Vincent, A.; Babu, S.; Brinley, E.; Karakoti, A.; Deshpande, S.; Seal, S. Role of Catalyst on Refractive Index Tunability of Porous Silica Antireflective Coatings by Sol−Gel Technique. *J. Phys. Chem. C* **2007**, *111*, 8291−8298.
(9) Wang, W. T.; Lu, N.; Hao, J. Y.; Xu, H. B.; Qi, D. P.; Chi, L. F. Self-Assembled Monolayer Islands Masked Chemical Etching for Broad-Band Antireflective Silicon Surfaces. *J. Phys. Chem. C* **2010**, *114*, 1989−1995.
(10) Hattori, H. Anti-Reflection Surface with Particle Coating Deposited by Electrostatic Attraction. *Adv. Mater.* **2001**, *13*, 51−54.
(11) Zarzycki, J. Past and Present of Sol-Gel Science and Technology. *J. Sol−Gel Sci. Technol.* **1997**, *8*, 17−22.
(12) Wheeler, E. K.; McWhirter, J. T.; Whitman, P. K.; Thorsness, C. B.; De Yoreo, J. J.; Thomas, I. M.; Hester, M. Scatter Loss from Environmental Degradation of KDP Crystals. *Proc. SPIE* **1999**, *3902*, 451−459.
(13) Smitha, S.; Shajesh, P.; Mukundan, P.; Warrier, K. G. K. Antiwetting Silica−Gelatin Nanohybrid and Transparent Nano Coatings Synthesised Through an Aqueous Sol−Gel Process. *J. Sol−Gel. Sci. Technol.* **2007**, *42*, 157−163.
(14) Yao, L. F.; Zhu, Y. G.; Qu, D.; Du, M. F.; Shen, J.; Wang, J. Optical and Hydrophobic Nano-Porous Silica Thin Films with Low Refractive Index. *Proc. SPIE* **2006**, *6034*, 225−231.
(15) Jeong, H. J.; Kim, D. K.; Lee, S. B.; Kwon, S. H.; Kadono, K. Preparation of Water-Repellent Glass by Sol−Gel Process Using Perfluoroalkylsilane and Tetraethoxysilane. *J. Colloid Interface Sci.* **2001**, *235*, 130−134.
(16) Pilotek, S.; Schmidt, H. K. Wettability of Microstructured Hydrophobic Sol-Gel Coatings. *J. Sol−Gel Sci. Technol.* **2003**, *26*, 789−792.
(17) Kim, S.; Zukoski, C. F. A Model of Growth by Hetero-Coagulation in Seeded Colloidal Dispersions. *J. Colloid Interface Sci.* **1990**, *139*, 198−212.
(18) Bogush, G. H.; Zukoski, C. F., IV Uniform Silica Particle Precipitation: An Aggregative Growth Model. *J. Colloid Interface Sci.* **1991**, *142*, 1−18.
(19) Ha, J. W.; Park, I. J.; Lee, S. B. Antireflection Surfaces Prepared from Fluorinated Latex Particles. *Macromolecules* **2008**, *41*, 8800−8806.
(20) Liu, R. L.; Xu, Y.; Wu, D.; Sun, Y. H.; Gao, H. C.; Yuan, H. Z.; Deng, F. Comparative Study on the Hydrolysis Kinetics of Substituted Ethoxysilanes by Liquid-State 29Si NMR. *J. Non-Cryst. Solids* **2004**, *343*, 61−70.
(21) Dirè, S.; Tagliazucca, V.; Callone, E.; Quaranta, A. Effect of Functional Groups on Condensation and Properties of Sol−Gel Silica Nanoparticles Prepared by Direct Synthesis from Organoalkoxysilanes. *Mater. Chem. Phys.* **2011**, *126*, 909−917.
(22) Zhang, Y.; Wu, D.; Sun, Y. H.; Peng, S. Y. The Hydrolysis-Polycondensation of MTES under Different Conditions and Its Applications. *Bull. Chin. Silic. Soc.* **2000**, *6*, 27−31.
(23) Floch, H. G.; Belleville, P. F. A Scratch-Resistant Single-Layer Antireflective Coating by a Low Temperature Sol-Gel Route. *J. Sol−Gel Sci. Technol.* **1994**, *1*, 293−304.
(24) Zhang, X. X.; Cai, S.; You, D.; Yan, L. H.; Lv, H. B.; Yuan, X. D.; Jiang, B. Template-Free Sol-Gel Preparation of Superhydrophobic ORMOSIL Films for Double-Wavelength Broadband Antireflective Coatings. *Adv. Funct. Mater.* **2013**, *23*, 4361−4365.
(25) Ma, Y.; Kanezashi, M.; Tsuru, T. Preparation of Organic/Inorganic Hybrid Silica Using Methyltriethoxysilane and Tetraethoxysilane as Co-precursors. *J. Sol−Gel. Sci. Technol.* **2010**, *53*, 93−99.